Performance Analysis of Analog Network Coding with Imperfect Channel Estimation in a Frequency-Selective Fading Channel

Haris Gacanin, Mika Salmela, and Fumiyuki Adachi

***Abstract*—Broadcast nature of the wireless channel enables wireless communications to make use of network coding at the physical layer (PNC) to improve the network capacity. Recently, narrowband and later broadband analog network coding (ANC) were introduced as a simpler implementation of PNC. The ANC schemes require two time slots while in PNC three time slots are required for bi-directional communication between two nodes and hence ANC is more spectrum efficient. The coherent detection and self-information removal in ANC require accurate channel state information (CSI). In this paper, we theoretically analyze the bit error rate (BER) performance with imperfect knowledge of CSI for broadband ANC using orthogonal frequency division multiplexing (OFDM), where the channel estimation error is modeled as a zero-mean complex Gaussian random variable. We investigate the BER performance for three cases: (i) the effect of imperfect self-information removal due to channel estimation (CE) error with fading tracking errors, (ii) the effect of imperfect self-information removal due to CE error without fading tracking errors, and (iii) the ideal CE case. We discuss how, and by how much, our results obtained by theoretical analysis can be used for design of broadband ANC system with the imperfect knowledge of CSI. Our results show that imperfect channel estimation due to the noise effect has less impact on self-information removal than the imperfect channel estimation due to fading tracking errors. The tracking against fading is an important problem for accurate self-information removal as well as coherent detection and thus, the effect of channel time-selectivity is also theoretically studied. The achievable BER performance gains due to the polynomial time-domain channel interpolation are investigated using the derived close-form BER expressions and it was shown that the broadband ANC schemes with practical CE in a time- and frequency-selective channel should include a more sophisticated channel interpolation techniques since the impact of Doppler shift has prevalent effect on the achievable BER performance.**

***Index Terms*—Broadband ANC, BER, theoretical analysis, channel estimation, OFDM.**

I. Introduction

NETWORK coding has been studied as a means to increase network capacity in wired networks [1]. In [2], [3], network coding was applied to wireless networks in order to achieve capacity gains due to broadcast nature of wireless channel. Narrowband physical layer network coding (PNC) schemes [4], [5] were shown to increase the capacity of bi-directional communication in a frequency-nonselective fading channel. To further improve the spectrum efficiency narrowband analog network coding (ANC), in [6], was introduced for communication over a frequency-nonselective fading channel without any processing at the relay which uses an amplify-and-forward (AF) scheme. However, in broadband wireless communications, the channel is frequency-selective, which renders schemes in [4]-[6] not applicable. Recently, broadband ANC scheme was presented for communication over a frequency-selective channel [7].

In broadband ANC scheme the coherent detection and self-information removal require accurate channel state information (CSI). The bit error rate (BER) performances with maximum likelihood (ML) channel estimation (CE) for narrowband ANC [8] and with two-slot pilot-assisted CE (PACE) for broadband ANC [9] were evaluated by computer simulation. In [9], it was shown that the BER performance with two-slot PACE is slightly degraded for low and moderate terminal speeds in comparison with ideal CE case. To our best knowledge, impact of imperfect knowledge of CSI on broadband ANC has not been well studied. We note that the CE error may degrade the BER performances of PNC and ANC schemes differently since PNC performs digital encoding at the packet level and its exact BER analysis in a frequency-selective channel may be very difficult if not impossible. In this work, we only consider the analysis of broadband ANC due to its higher spectrum efficiency.

In this paper, we present the BER performance analysis of bi-directional broadband ANC in a frequency-selective fading channel. We derive a closed-form BER expression using orthogonal frequency division multiplexing (OFDM) radio access with imperfect knowledge of CSIs, where the CE error is modeled as a zero-mean complex Gaussian random variable. In our analysis we investigate the BER performance for three cases: (i) the effect of imperfect self-information removal due to CE error with fading tracking errors, (ii) the effect of imperfect self-information removal due to CE error without fading tracking errors, and (iii) the ideal CE case. We discuss how, and by how much, the achievable BER performance is affected by the CE error with imperfect channel tracking and the imperfect self-information removal. We also discuss how the results obtained by theoretical analysis can be used to design the broadband ANC system with imperfect knowledge of CSI. Our results show that the imperfect CE due to the additive noise effect has less impact on self-information removal than the imperfect CE due to fading tracking error, which is also

Manuscript received February 21, 2011; revised August 29, 2011; accepted November 29, 2011. The associate editor coordinating the review of this paper and approving it for publication was K. K. Wong.

Some limited results of this paper are presented in IEEE International Conference on Communication Systems 2010 [12]. In the conference version [12], however, the complete derivation of the exact BER for broadband ANC with imperfect channel estimation and channel tracking is not presented.

H. Gacanin is with the Motive Division, Alcatel-Lucent Bell N.V., Antwerp, Belgium (e-mail: harisg@ieee.org).

M. Salmela is with the School of Science and Technology, Aalto University, Aalto, Finland.

F. Adachi is with the Graduate School of Engineering, Tohoku University, Sendai, Japan.

Digital Object Identifier 10.1109/TWC.2011.122211.110326

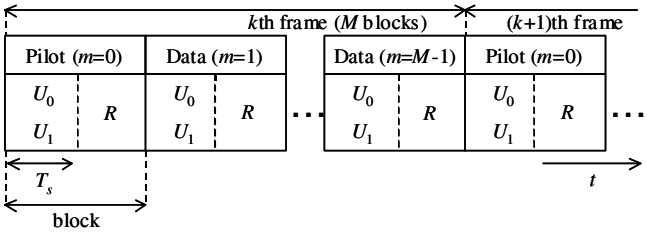

Fig. 1. Frame structure.

theoretically studied. The achievable BER performance gains due to the polynomial time-domain channel interpolation are investigated using the derived close-form BER expressions to show that the broadband ANC system should include a more sophisticated channel interpolation techniques since the impact of Doppler shift has prevalent effect on the achievable BER performance.

The remainder of this paper is organized as follows. In Section II, we present the network model. The performance analysis is presented in Section III, while the numerical results and discussions are presented in Sect. IV. The conclusion is set out in Section V.

II. Network Model

This section is devoted in part to definition of the multipath channel and the ANC signal transmission. We consider a bi-directional network with relay R and two users U_0 and U_1 that are assumed to be out of each other's transmission range. The transmission frame structure is illustrated in Fig. 1. Each frame consists of M blocks, where the first block ($m = 0$) is used for pilot-assisted CE. The communication between two users in the mth block takes place during two slots; (i) in the first slot ($q = 0$) the users simultaneously transmit to the relay (ii) during the second slot ($q = 1$) the relay broadcasts the received signals to both users using an amplify-and-forward protocol.

Without loss of generality, below we consider the mth block transmission in a frame.

A. Channel Model

The propagation channel over a frame is characterized by the impulse response given by

$$h_{q,j,m}(\tau) = \sum_{l=0}^{L-1} h_{q,j,m}(l)\delta(\tau - \tau_l), \tag{1}$$

where L denotes the number of paths, $h_{q,j,m}(l)$ denotes the path gain between the relay R and jth user U_j at slot q ($q \in \{0, 1\}$) during the mth block of kth frame, $\delta(\cdot)$ denotes the delta function and τ_l denotes the time delay of the lth path. Without loss of generality, we assume $\tau_0 = 0 < \tau_1 < \cdots < \tau_{L-1}$ and that the lth path time delay is $\tau_l = l\Delta$, where Δ (≥ 1) denotes the time delay separation between adjacent paths. The guard interval (GI) is assumed to be longer than the maximum channel time delay. The shadowing and distance-dependent path loss are not considered in this model for the sake of brevity.

We consider the Jakes fading model, where incoming rays constituting each propagation path arrive at a user with uniformly distributed angles [10]. Thus, the normalized autocorrelation function of a Rayleigh faded channel with motion at a constant velocity is given by $R(\varsigma) = E[h_{q,j,m}h^*_{q,j,m+\varsigma}] = J_0(2\pi f_D \varsigma)$ at delay ς when the maximum Doppler shift is f_D, where $J_0(\alpha) = \frac{1}{\pi}\int_0^{\pi} \exp(j\alpha\cos\phi)d\phi$ is the 0^{th} order Bessel function of first kind. We also consider the block fading, where the fading gains remain constant during one block and vary block-by-block within the frame. The channel gain at the nth subcarrier is given as an output of Fourier transform operation represented by $H_{q,j,m}(n) = \sum_{\tau=0}^{L-1} h_{q,j,m}(\tau)\exp\{-j2\pi n\frac{\tau}{N_c}\}$ for $n = 0 \sim N_c - 1$.

B. Transmission Signal Representation

The jth ($j \in \{0, 1\}$) user's data block symbol sequence $\{d_{j,m}(n);\ n = 0 \sim N_c - 1\}$ is fed to an N_c-point inverse fast Fourier transform (IFFT) to generate the jth user's time-domain OFDM signal $\{s_{j,m}(t); t = 0 \sim N_c - 1\}$. Then, an N_g-sample guard interval (GI) is added and the GI-added OFDM signal is transmitted over a time-varying frequency-selective fading channel.

First time slot (q=0): By assuming perfect time and frequency synchronization at the relay, during the first time slot (TS_0), the nth subcarrier component can be expressed as

$$\begin{aligned} R_{r,m}(n) \ &= \sqrt{P}d_{0,m}(n)H_{0,0,m}(n) \\ &\quad +\sqrt{P}d_{1,m}(n)H_{0,1,m}(n) + N_{r,m}(n), \end{aligned} \tag{2}$$

for $n = 0 \sim N_c - 1$, where $H_{q,j,m}(n)$ and $N_{r,m}(n)$, respectively, denote the Fourier transforms of the channel impulse response during the mth block between U_j and R and the zero mean additive white Gaussian noise (AWGN) having power spectral density N_0. In the above expression P represents the signal transmit power. The received signal given by (2) is amplified and broadcasted over a frequency-selective fading channel. For the sake of the analysis we normalize the transmit signal by a factor β, which is the square root of the average received signal power plus noise power.

Second time slot (q=1): During the second slot, by assuming perfect time and frequency synchronization, the received signal at the jth user U_j after FFT can be expressed as

$$R_{j,m}(n) = \frac{\sqrt{P}}{\beta}R_{r,m}(n)H_{1,j,m}(n) + N_{j,m}(n) \tag{3}$$

for $n = 0 \sim N_c - 1$, where $N_{j,m}(n)$ is the zero-mean noise having variance N_0/T_s due to the AWGN. The jth user U_j removes its self-information as

$$\tilde{R}_{j,m}(n) = R_{j,m}(n) - \frac{P}{\beta}d_{j,m}(n)H_{0,j,m}(n)H_{1,j,m}(n). \tag{4}$$

Finally, the decision variables of the jth user U_j are given by

$$\hat{d}_{j,m}(n) = \tilde{R}_{j,m}(n)w_{j,m}(n) \tag{5}$$

for $n = 0 \sim N_c - 1$, where $w_{j,m}(n)$ denotes the maximum ratio combining (MRC) frequency domain equalization weight given by $w_{j,m}(n) = H^*_{0,\bar{j},m}(n)H^*_{1,j,m}(n)$. Note that $\bar{A}$ represents the logical negation (i.e., logical 'NOT' operation) of A.

III. Performance Analysis

We first establish a mathematical definition of the channel estimation error and then, we develop a mathematical model for the closed-form BER expressions with quadrature phase shift keying (QPSK) data modulation. We also analytically evaluate the impact of channel time-selectivity on the BER performance with practical pilot-assisted CE scheme [9]. Finally, the closed-form BER expression for broadband ANC with perfect knowledge of CSI is also presented. Without loss of generality we only consider the derivation of BER expressions for the jth user U_j for the sake of brevity.

The transmission frame structure, where the kth frame constitutes of one pilot block and M-1 data blocks, is illustrated in Fig. 1. The block fading channel model is assumed, where the fading gains remain constant during one block, but vary block-by-block within the frame.

A. CE Error Model

The estimated channel gains for the mth block within the kth frame can be represented as

$$\bar{H}^k_{q,j,0}(n) = H^k_{q,j,0}(n) + \epsilon^k_{q,j,0}(n) \tag{6}$$

where $\epsilon^k_{q,j,m}(n)$ is the channel estimation error. We model the channel estimation error $\epsilon^k_{q,j,m}(n)$ as independent identically distributed zero-mean complex Gaussian random variable with the variance given by σ_e^2.

B. Impact of CE Error with Fading Tracking Errors

In this subsection, we only consider the kth frame transmission with the $zero$th order channel time interpolation (i.e., the channel estimate obtained by a pilot block is used for detection of succeeding M-1 data blocks in a frame). Thus, without loss of generality, in this subsection the frame index k is omitted from (6) for the sake of brevity.

The coherent detection in the mth OFDM data block given by (5) can be expressed as

$$\hat{d}_{j,m}(n) = X_{j,m}(n)Y^*_{j,m}(n) \tag{7}$$

for $n = 0 \sim N_c - 1$, where

$$\begin{cases} X_{j,m}(n) &= \frac{P}{\beta} d_{\bar{j},m}(n) H_{sd,m}(n) \\ &\quad + \frac{\sqrt{P}}{\beta} H_{1,j,m}(n) N_{r,m}(n) + N_{j,m}(n) \\ &\quad + \frac{P}{\beta} d_{j,m}(n) H_{d,m}(n) - \frac{P}{\beta} d_{j,m}(n) H_{d,0}(n) \\ &\quad - \frac{P}{\beta} d_{j,m}(n) \epsilon_x(n) \\ Y_{j,m}(n) &= H_{sd,m}(n) + \epsilon_y(n) \end{cases} \tag{8}$$

and

$$\begin{cases} H_{sd,m}(n) = H_{0,\bar{j},m}(n) H_{1,j,m}(n), \\ H_{d,m}(n) = H_{0,j,m}(n) H_{1,j,m}(n), \\ \epsilon_x(n) = H_{0,j,0}(n)\epsilon_{1,j,0}(n) \\ \qquad + \epsilon_{0,j,0}(n) H_{1,j,0}(n) + \epsilon_{0,j,0}(n)\epsilon_{1,j,0}(n), \\ \epsilon_y(n) = H_{0,\bar{j},0}(n)\epsilon_{1,j,0}(n) \\ \qquad + \epsilon_{0,\bar{j},0}(n) H_{1,j,0}(n) + \epsilon_{0,\bar{j},0}(n)\epsilon_{1,j,0}(n), \end{cases} \tag{9}$$

where $H_{sd,m}(n)$ denotes channel gain at the nth subcarrier that the signal experiences from source to destination terminal, while $H_{d,m}(n)$ denotes the channel gain experienced by the self-information term.

In this paper, we assume that $\epsilon_{q,j,m}(n)$ are independent zero-mean complex Gaussian random variables. Thus, for the given channel gains $\{H_{0,j,0}(n)\}$ and $\{H_{1,j,0}(n)\}$, we assume that the terms $H_{0,j,0}(n)\epsilon_{1,j,0}(n)$ and $\epsilon_{0,j,0}(n)H_{1,j,0}(n)$ as well as $H_{0,\bar{j},0}(n)\epsilon_{1,j,0}(n)$ and $\epsilon_{0,\bar{j},0}(n)H_{1,j,0}(n)$ are also independent complex Gaussian random variables. However, the cross terms $\epsilon_{0,j,0}(n)\epsilon_{1,j,0}(n)$ and $\epsilon_{0,\bar{j},0}(n)\epsilon_{1,j,0}(n)$ are not a Gaussian variables, but most of the time it can be assumed that they are much smaller than $H_{0,j,0}(n)\epsilon_{1,j,0}(n) + \epsilon_{0,j,0}(n)H_{1,j,0}(n)$ and $H_{0,\bar{j},0}(n)\epsilon_{1,j,0}(n) + \epsilon_{0,\bar{j},0}(n)H_{1,j,0}(n)$ and therefore, can be neglected. Thus, $\epsilon_x(n)$ and $\epsilon_y(n)$ are assumed to be independent (i.e., $E[\epsilon_y(n)\epsilon_y(n)] = 0$) zero-mean complex Gaussian random variables. Consequently, for the given channel gain $\{H_{q,j,m}(n)\}$ both $X_{j,m}(n)$ and $Y_{j,m}(n)$ for $n = 0 \sim N_c - 1$ are zero-mean complex Gaussian random variables. We note here that exact BER derivation taking into consideration the cross-terms $\epsilon_{0,j,0}(n)\epsilon_{1,j,0}(n)$ and $\epsilon_{0,\bar{j},0}(n)\epsilon_{1,j,0}(n)$ is very difficult if not impossible. Thus, the jth user's BER within the mth frame can be represented as [11]

$$P_{4b,m} = P[Re[X_{j,m}(n)Y^*_{j,m}(n)] < 0] = \frac{1}{2}\left[1 - \frac{\mu}{\sqrt{2-\mu^2}}\right], \tag{10}$$

where $P[a]$ and μ, respectively, denote the probability of a and the normalized covariance given as

$$\mu = \frac{Re[g_{xy}]}{\sqrt{g_{xx}g_{yy} - Im[g_{xy}]^2}} \tag{11}$$

with the second moments

$$\begin{cases} g_{xx} &= E[|X_{j,m}(n)|^2], \\ g_{yy} &= E[|Y_{j,m}(n)|^2], \\ g_{xy} &= E[X_{j,m}(n)Y^*_{j,m}(n)]. \end{cases} \tag{12}$$

Since

$$\begin{cases} E[|H_{q,j,m}(n)|^2] = 1, \\ E[H_{q,j,m}(n)H^*_{q,j,0}(n)] = J_0(2\pi f_D T_s m), \\ E[|N_{j,m}(n)|^2] = E[|N_{r,m}(n)|^2] = 2\sigma_n^2, \\ E[|\epsilon_{q,j,m}(n)|^2] = 2\sigma_e^2, \end{cases} \tag{13}$$

we obtain [Appendix]

$$\begin{cases} g_{xx} &= 2\frac{P^2}{\beta^2} + \frac{P^2}{\beta^2}(1+2\sigma_e^2)^2 \\ &\quad - 2\frac{P^2}{\beta^2} J_0^2(2\pi f_D T_s m) + (\frac{P}{\beta^2}+1)2\sigma_n^2, \\ g_{yy} &= (1+2\sigma_e^2)^2, \\ g_{xy} &= \frac{P}{\beta} J_0^2(2\pi f_D T_s m). \end{cases} \tag{14}$$

In the above expressions σ_e^2 denotes the variance of channel estimation error $\epsilon_{q,j,m}(n)$ and $\sigma_n^2 = N_0/T_s$ is the noise power due to AWGN with $1/T_s$ being data symbol rate. From (14) it can be seen that g_{xx} and g_{xy} are a function of the frame index m. This is due to the fact that the CE is done only at position $m = 0$ and the same channel estimates are used for the following blocks with $m \neq 0$. As the cross-correlation term g_{xy} is a real number and thus, (11) reduces to

$$\mu = \frac{g_{xy}}{\sqrt{g_{xx}g_{yy}}}. \tag{15}$$

Using (14), (11) and (10) the normalized covariance μ [Appendix] and $P_{4b,m}$ are shown as (16) and (17), respectively, at the top of the next page. The second moments in (14)

are derived by taking ensemble average over fading statistics. Thus, g_{xy}, g_{xx} and g_{yy} are not a function of the user index j. Consequently, the BER given by (17) is the same for both users U_0 and U_1. Using (17) the average BER expression for the OFDM frame is finally calculated by averaging the $M-1$ data blocks as $P_{4b} = \sum_{m=1}^{M-1} P_{4b,m}$.

C. BER with Polynomial Interpolation

The channel time-selectivity is a very important problem in practice. Here, the BER expressions with pilot-assisted CE scheme using polynomial interpolation are derived to evaluate the impact of channel time-selectivity on the BER performance of broadband ANC.

The BER performance with polynomial interpolation is affected by the channel time-selectivity. The analysis of BER performance with interpolation takes into consideration different transmission frames. Thus, in this subsection, we take into consideration the frame index k and the channel estimates in the first block ($m = 0$) of the kth frame are given by (6).

The channel estimates are obtained from the pilot signal, which is transmitted in the first block (i.e., $m = 0$) of the each frame as shown in Fig. 1. Blocks are divided into two stages, corresponding to the first and second time slot, TS_0 and TS_1, respectively, each consisting of $N_c + N_g$ samples (i.e., duration of T_s). In the first time slot TS_0, the users U_0 and U_1, respectively transmit their pilot signals, $p_0(t)$ and $p_1(t) = p_0((t-\Delta) mod N_c)$, where Δ denotes the time shift [9]. The relay estimates the channel gains and in the second time slot TS_1 broadcasts its pilot signal $p_0(t)$ to both users. Finally, the users estimate the corresponding channel gains using the broadcasted pilot signal in TS_1 of the first block. The estimated CSIs obtained from the pilot block are used in detecting the following $M-1$ data blocks within the kth frame. We note here that more details about the CE scheme can be found in [9].

1) First order interpolation: The first order interpolated channel gain $\bar{H}^k_{q,j,m}(n)$ of the kth frame at the mth block is obtained as

$$\begin{aligned}\bar{H}^k_{q,j,m}(n) &= \tfrac{M-m}{M}[H^k_{q,j,0}(n) + \epsilon^k_{q,j,0}(n)] \\ &\quad + \tfrac{m}{M}[H^{k+1}_{q,j,0}(n) + \epsilon^{k+1}_{q,j,0}(n)].\end{aligned} \tag{18}$$

Using (18) with (28) and (29) in Appendix the second moments g_{xy}, g_{xx} and g_{yy} for the first order interpolation can be represented by

$$\begin{cases} g_{xx} &= 2\frac{P_s^2}{\beta^2} + (\frac{P}{\beta^2}+1)2\sigma_n^2 + \frac{P_s^2}{\beta^2}A_1 + \frac{P_s^2}{\beta^2}g_{yy}, \\ g_{yy} &= \left[(\frac{M-m}{m})^2 + (\frac{M}{m})^2\right]^2(1+2\sigma_e^2)^2 \\ &\quad +4(\frac{M-m}{m})^3(\frac{M}{m})(1+2\sigma_e^2)J_0(2\pi f_D T_s M) \\ &\quad +4(\frac{M-m}{m})(\frac{M}{m})^3(1+2\sigma_e^2)J_0(2\pi f_D T_s M) \\ &\quad +4(\frac{M-m}{m})^2(\frac{M}{m})^2 J_0^2(2\pi f_D T_s M), \\ g_{xy} &= \frac{P}{\beta}A_2, \end{cases} \tag{19}$$

where A_1 and A_2 for the sake of brevity are given as (33) in Appendix. It can be seen in (19) that g_{xx} and g_{xy} are also functions of the frame index m and consequently, the channel time-selectivity.

2) Second order interpolation: The second order interpolated channel gain $\bar{H}^k_{q,j,m}(n)$ of the kth frame at the mth block is obtained as

$$\begin{aligned}\bar{H}^k_{q,j,m}(n) &= \tfrac{(M-m)(m-2M)}{2M^2}[H^k_{q,j,0}(n) + \epsilon^k_{q,j,0}(n)] \\ &\quad + \tfrac{m(2M-m)}{M}[H^{k+1}_{q,j,0}(n) + \epsilon^{k+1}_{q,j,0}(n)] \\ &\quad + \tfrac{m(m-M)}{2M^2}[H^{k+2}_{q,j,0}(n) + \epsilon^{k+2}_{q,j,0}(n)],\end{aligned} \tag{20}$$

which leads to

$$\begin{cases} g_{xx} &= 2\frac{P_s^2}{\beta^2} + (\frac{P}{\beta^2}+1)2\sigma_n^2 + \frac{P_s^2}{\beta^2}A_1 + \frac{P_s^2}{\beta^2}g_{yy}, \\ g_{yy} &= \big[(\frac{(M-m)^4(2M-m)^4}{16M^8} + \frac{m^4(2M-m)^4}{M^8} \\ &\quad + \frac{m^4(m-M)^4}{16M^8} + \frac{m^2(m-M)^4(2M-m)^2}{8M^8} \\ &\quad + \frac{m^4(m-M)^2(2M-m)^2}{2M^8} \\ &\quad + \frac{m^2(m-M)^2(2M-m)^4}{2M^8}\big](1+2\sigma_e^2)^2 \\ &\quad + J_0(2\pi f_D T_s M)B_1 + J_0(2\pi f_D T_s 2M)B_2 \\ g_{xy} &= \frac{P}{\beta}A_2, \end{cases} \tag{21}$$

where A_1, A_2, B_1 and B_2 are given by (34) in Appendix. Here it can be seen that g_{xx} and g_{xy} are also a function on the frame index m as shown for the first order interpolation case.

3) BER Evaluation: Substituting the second moments to (15) we obtain

$$\mu = \frac{A_2}{\sqrt{(2 + (\frac{E_s}{2N_0})^{-1} + (\frac{E_s}{2N_0})^{-2} + A_1 + g_{yy})g_{yy}}}. \tag{22}$$

Thus, the BER performance for broadband ANC with first and second order interpolation schemes is finally derived as

$$P_{4b,m} = \frac{1}{2}\left[1 - \frac{A_2}{\sqrt{(4+2(\frac{E_s}{2N_0})^{-1}+2(\frac{E_s}{2N_0})^{-2}+2A_1+2g_{yy})g_{yy} - A_2^2}}\right]. \tag{23}$$

Next we present a closed-form BER for broadband ANC with perfect knowledge of CSI (i.e., ideal CE case).

D. Exact BER Analysis with Perfect Knowledge of CSI

In the case of perfect knowledge of CSI the channel estimation error is not present and (14) collapses to

$$\begin{cases} g_{xx} &= \frac{P^2}{\beta^2} + (\frac{P}{\beta^2}+1)2\sigma_n^2, \\ g_{yy} &= 1, \\ g_{xy} &= \frac{P}{\beta}, \end{cases} \tag{24}$$

and after some manipulations the average BER is given by

$$P_{4b} = \frac{1}{2}\left[1 - \frac{1}{\sqrt{1 + 2(\frac{E_s}{2N_0})^{-1} + 2(\frac{E_s}{2N_0})^{-2}}}\right]. \tag{25}$$

IV. Numerical Results and Discussions

The numerical simulation parameters are shown in Table I. We assume ideal coherent QPSK modulation/demodulation with $N_c = 256$ and GI length of $N_g = 32$. The propagation channel is an L-path Rayleigh fading channel, where the path gains $\{h_{q,l,j,m}; l = 0 \sim L-1\}$ are zero-mean independent complex variables with $E[|h_{q,l,j,m}|^2] = 1/L$. The maximum time delay of the channel is assumed to be less than the guard interval and that all paths are independent of each other. $f_D T_s$ denotes the normalized Doppler frequency, where $1/T_s$ is the transmission symbol rate ($f_D T_s = 10^{-3}$ corresponds to a

$$\mu = \frac{J_0^2(2\pi f_D T_s m)}{\sqrt{(2+(1+2\sigma_e^2)^2 - 2J_0^2(2\pi f_D T_s m) + (\frac{E_s}{2N_0})^{-1} + (\frac{E_s}{2N_0})^{-2})(1+2\sigma_e^2)^2}} \tag{16}$$

$$P_{4b,m} = \frac{1}{2}\left[1 - \frac{J_0^2(2\pi f_D T_s m)}{\sqrt{(4+2(1+2\sigma_e^2)^2 - 4J_0^2(2\pi f_D T_s m) + 2(\frac{E_s}{2N_0})^{-1} + 2(\frac{E_s}{2N_0})^{-2})(1+2\sigma_e^2)^2 - J_0^4(2\pi f_D T_s m)}}\right] \tag{17}$$

TABLE I
NUMERICAL SIMULATION PARAMETERS.

Transmitter	Data modulation	QPSK
	Block size	$N_c = 256$
	GI	$N_g = 32$
Channel	L-path block Rayleigh fading with $\Delta = 1$	
Receiver	FDE	MRC

mobile terminal speed of approximately 80 km/h for a transmission data rate of 100 Msymbols/s and a carrier frequency of 5GHz). Distance-dependent path loss and shadowing loss are not considered.

A. Impact of CE Error and Imperfect Self-information Removal

We first evaluate the impact of CE error on the BER performance and then, the derived theoretical expressions are used to evaluate the impact of imperfect self-information removal due to CE errors. Figure 2 illustrates the impact of channel estimation error on the BER performance of broadband ANC in a frequency-selective fading channel with $zero$th order channel time interpolation. The BER performance as a function of the average signal energy per bit-to-AWGN power spectrum density ratio E_b/N_0 $(= 0.5(E_s/N_0)(1 + N_g/N_c))$ with $f_D T_s = 0$ and σ_e^2 as a parameter is illustrated in Fig. 2(a). The results shows that for the values less than $\sigma_e^2 = 10^{-4}$ the BER performance with imperfect and perfect CSI can be considered fairly equal. On the other hand, it can be seen from the figure that for σ_e^2 larger than 10^{-4} the BER floor is observed. As the value of σ_e^2 increases from 10^{-3} to 10^{-2} and 10^{-1} the BER floor increases to about 3×10^{-3}, 3×10^{-2} and 2×10^{-1}, respectively. A good agreement between the analytical approach and computer simulation can be seen from the figure.

Figure 2(b) illustrates the BER performance as a function of channel estimation error variance σ_e^2 with $f_D T_s$ as a parameter. We consider three cases: (i) the effect of imperfect self-information removal due to CE error with fading tracking errors which is labeled as "Imperfect CSI $(f_D T_s = 10^{-3})$", (ii) the effect of imperfect self-information removal due to CE error without fading tracking errors, which is labeled as "Imperfect CSI $(f_D T_s = 0)$" and (iii) the ideal CE case. It was shown that for $\sigma_e^2 = 10^{-4}$, the CE error due to AWGN has less impact on self-information removal than fading tracking errors, which is labeled as "Imperfect CSI $(f_D T_s = 10^{-3})$". Thus, the broadband ANC system should be designed to be more robust to the channel time variation with a careful selection of the pilot insertion interval M. This issue is elaborated in the following.

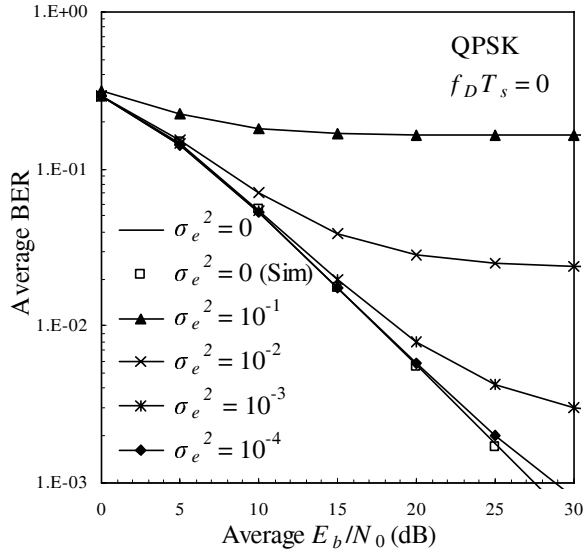

(a) Impact of σ_e^2.

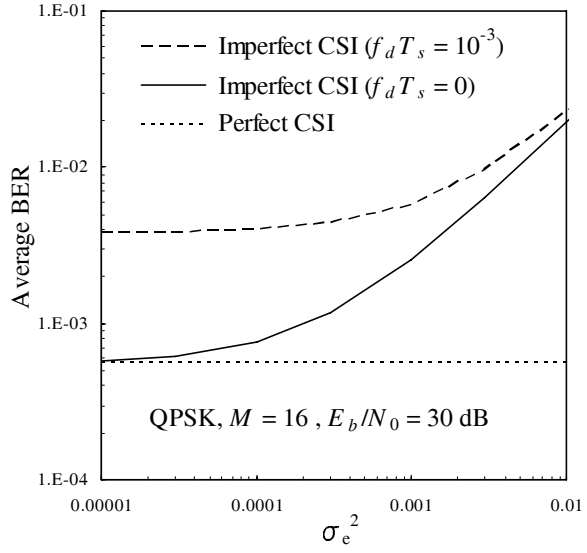

(b) Effect of self-information removal on BER.

Fig. 2. Impact of channel estimation error on BER performance.

B. Impact of Pilot Insertion Rate

Figures 3(a) and 3(b) illustrate the average BER performance as a function of the average E_b/N_0 with the frame size M as a parameter with (i.e., $\sigma_e^2 = 10^{-3}$) and without (i.e., $\sigma_e^2 = 0$) CE error. It can be seen from the figure that as the frame size M increases and the difference between actual channel gain and its estimate used in self-information removal gets larger the resulting self-interference increases which causes the BER performance degradation.

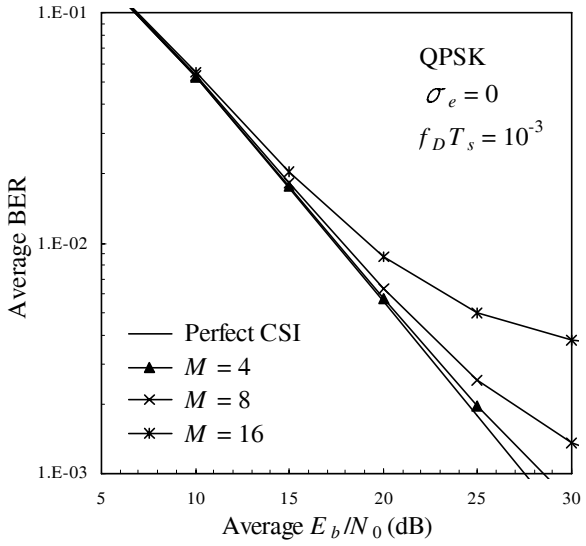

(a) Impact of frame size with $\sigma_e^2 = 0$.

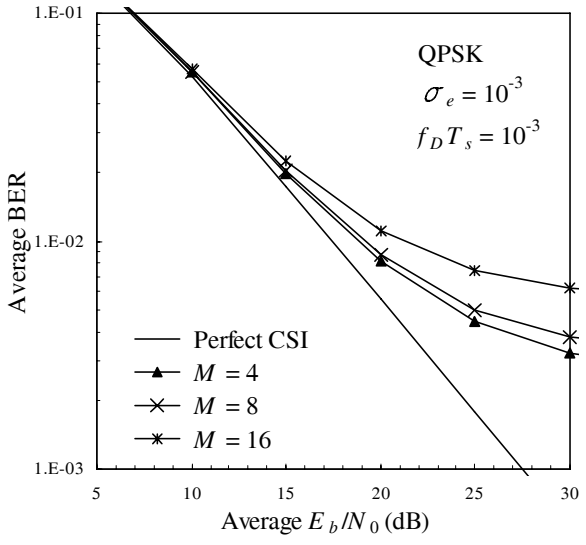

(b) Impact of frame size with $\sigma_e^2 \neq 0$.

Fig. 3. Impact of frame size on BER performance.

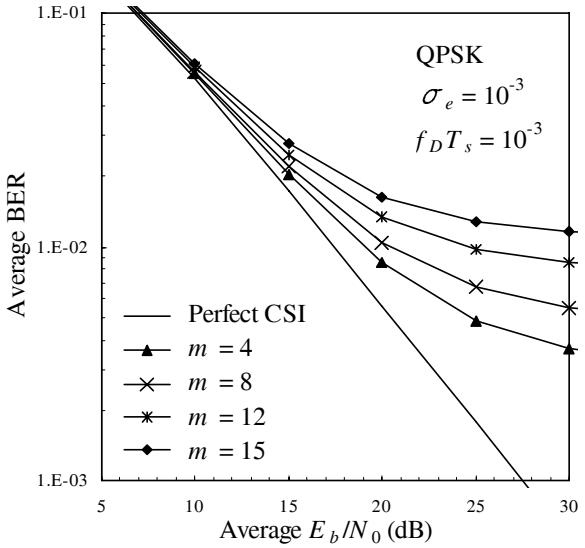

Fig. 4. BER performance of individual block m within the frame.

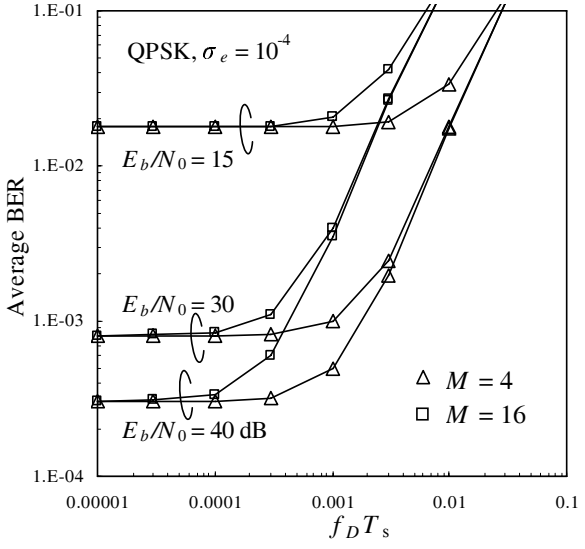

Fig. 5. Impact of $f_D T_s$.

Figure 4 illustrates the BER performance of the mth block within the kth frame as a function of the average E_b/N_0 when $\sigma_e^2 = 10^{-3}$. The figure shows that the larger the block index m is, the BER performance with imperfect knowledge of CSI is more degraded. This is because the channel gains at the end of the frame vary from the channel gains at the pilot block $(m = 0)$ due to the channel time-selectivity.

Figure 5 shows the BER performance as a function of $f_D T_s$ with E_b/N_0 as a parameter when $\sigma_e^2 = 10^{-4}$. The general behavior of the plots is that BER increases as the Doppler spread increases. The reason is the existence of severe ICI caused by self-information removal due to Doppler shifts as indicated in Fig. 2(b). Another observation from this plot is that if the value of $f_D T_s$ is below 10^{-4} (corresponding to a vehicle moving at a speed of about 8km/h for a carrier frequency of 5GHz) the BER degradation is negligible. However, as $f_D T_s$ increases (i.e., higher vehicular speeds), the channel time-selectivity clearly has a larger impact on the BER performance due to tracking errors then the AWGN and consequently, an improved channel estimation scheme using either time-domain interpolation or decision feedback must be designed to better cope with the Doppler shift.

C. Impact of the Channel Time-selectivity

Figure 6(a) shows the BER performance of broadband ANC with the first-order channel interpolation as a function of E_b/N_0 with $f_D T_s$ as a parameter with $\sigma_e^2 = 10^{-3}$ and $M = 16$. Our simulations were performed for three different values of the OFDM-symbol normalized Doppler frequency, namely for $f_D T_s$=0.03, 0.01 and 0.001. It can be seen that the performance of the system without time-domain interpolation is indeed tolerant to the Doppler frequency for the mobile user velocity of about 80 km/h (corresponding to the normalized Doppler frequency $f_D T_s = 10^{-3}$ for a carrier frequency of 5GHz). On the other hand, for the mobile user velocity of about 800 km/h (corresponding to the normalized Doppler frequency $f_D T_s = 10^{-2}$ for a carrier frequency of 5GHz) the significant BER performance improvement is observed

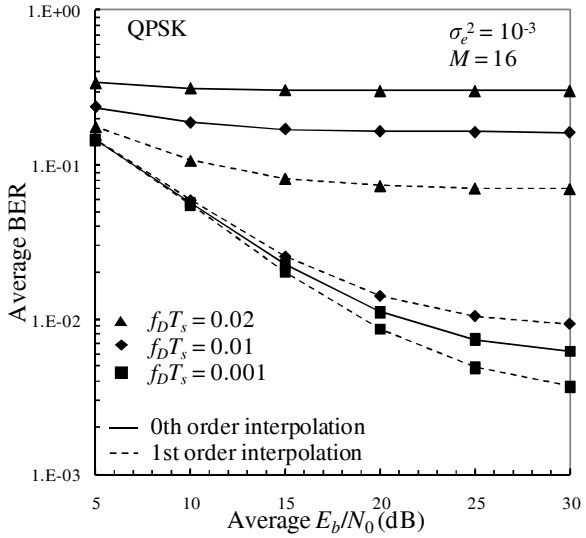

(a) 1^{st} order interpolation.

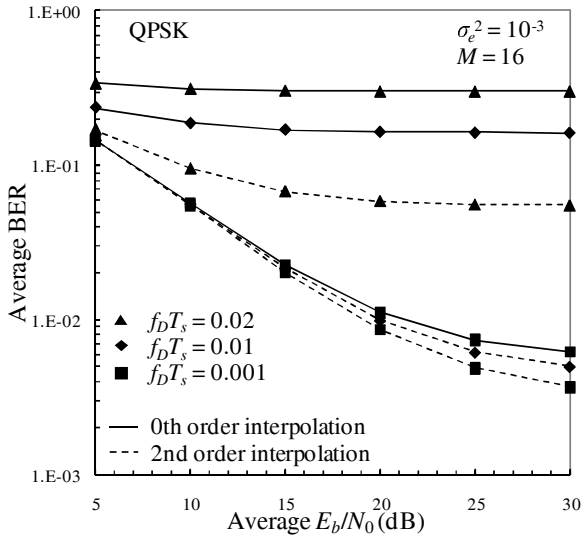

(b) 2^{nd} order interpolation.

Fig. 6. BER performance using polynomial interpolation.

in comparison with the CE case where interpolation is not used (i.e., 0^{th} order). However, for a higher mobile user velocity (corresponding to the normalized Doppler frequency $f_DT_s = 10^{-1}$ for a carrier frequency of 5GHz) a BER floor is observed due to a fast fading variation that cannot be tracked by the first-order interpolation.

Figure 6(b) shows the BER performance of broadband ANC using pilot-assisted CE with the second-order interpolation as a function of E_b/N_0 with f_DT_s as a parameter. The values of σ_e^2 and M are same as in Fig. 6(a). For the the mobile user speed of about 80 km/h (i.e., normalized Doppler frequency $f_DT_s = 10^{-3}$ for a carrier frequency of 5GHz) the second-order interpolation slightly improves the BER performance in comparison with the CE case when the first-order interpolation. The larger BER performance gain with the second-order interpolation can be observed for the mobile user velocity of about 800 km/h (i.e., normalized Doppler frequency $f_DT_s = 10^{-2}$ for a carrier frequency of 5GHz), while for the higher velocity (corresponding to the normalized Doppler frequency $f_DT_s = 10^{-1}$ for a carrier frequency of 5GHz) the BER performance severely degrades since the channel fluctuations are too fast and they cannot be encountered by the polynomial interpolation. Furthermore, it can be confirmed from Fig. 6 that the channel time-selectivity have a stronger impact on the performance of broadband ANC with imperfect knowledge of CSI in comparison with the effect of CE error discussed above.

In general, this suggests that the broadband ANC schemes with practical CE in a time- and frequency-selective channel should include a more sophisticated channel interpolation techniques since the impact of Doppler shift has prevalent effect on the achievable BER performance.

V. Conclusion

In this paper, we presented the closed-form BER expressions for bi-directional ANC with imperfect knowledge of CSI in a frequency-selective fading channel. In this paper, the Gaussian model of channel estimation error was used. We discussed the impact of imperfect self-information removal and the channel tracking on the achievable BER performance. The results with the $zero$th order channel time interpolation show that the imperfect CE due to AWGN has less impact on self-information removal than the imperfect channel tracking (i.e., fading tracking error). To improve the tracking ability, polynomial interpolation can be used. The BER expressions with pilot-assisted CE scheme using polynomial interpolation were also derived to evaluate impact of the channel time-selectivity. It was shown that the BER performance of broadband ANC with polynomial interpolation is more robust against the negative effect of channel time-selectivity and CE errors that cause imperfect self-information removal.

Further performance improvements can be obtained by using a higher order interpolation techniques, but their analysis may become very difficult if not impossible to track. Development of pilot-assisted CE for bi-directional ANC with improved fading tracking ability is an important future study. The performance analysis and comparison of ANC and PNC with pilot-assisted CE is also left as an interesting future work.

Acknowledgment

This work was supported in part by 2010 KDDI Foundation Research Grant Program.

Appendix

In this appendix we give some details on derivation of second moments and normalized covariance for broadband ANC with imperfect knowledge of CSI. We assume the $zero$th order channel time interpolation over M observed blocks within the frame.

A. Decision Variables

The received signal at the $j$the user U_j is given by

$$\begin{aligned} R_{j,m}(n) &= \frac{P}{\beta} d_{j,m}(n) H_{0,j,m}(n) H_{1,j,m}(n) \\ &+ \frac{P}{\beta} d_{\bar{j},m}(n) H_{0,\bar{j},m}(n) H_{1,j,m}(n) \\ &+ \frac{\sqrt{P}}{\beta} N_{r,m}(n) H_{1,j,m}(n) + N_{j,m}(n) \quad (26) \end{aligned}$$

for $n = 0 \sim N_c - 1$, while the signal after imperfect self-information removal due to CE error is given by

$$\begin{aligned}\tilde{R}_{j,m}(n) &= R_{j,m}(n) \\ &- \frac{P}{\beta} d_{j,m}(n)\bar{H}_{0,j,m}(n)\bar{H}_{1,j,m}(n), \end{aligned} \quad (27)$$

where the channel estimates are represented by $\bar{H}_{s,j,m}(n) = H_{s,j,0}(n)+\epsilon_{s,j,0}(n)$. Finally, after some manipulation, the decision variables for broadband ANC with imperfect knowledge of CSI are given by

$$\begin{aligned}\tilde{R}_{j,m}(n) &= X_{j,m} = \frac{P}{\beta} d_{j,m}(n)H_{0,j,m}(n)H_{1,j,m}(n) \\ &- \frac{P}{\beta} d_{j,m}(n)H_{0,j,0}(n)H_{1,j,0}(n) \\ &+ \frac{P}{\beta} d_{\bar{j},m}(n)H_{0,\bar{j},m}(n)H_{1,j,m}(n) \\ &+ \frac{\sqrt{P}}{\beta} N_{r,m}(n)H_{1,j,m}(n) + N_{j,m}(n) \\ &- \frac{P}{\beta} d_{j,m}(n)H_{0,j,0}(n)\epsilon_x(n) \end{aligned} \quad (28)$$

for $n = 0 \sim N_c - 1$, where $\epsilon_x(n) = H_{0,j,0}(n)\epsilon_{1,j,0}(n) + H_{1,j,0}(n)\epsilon_{0,j,0}(n) + \epsilon_{0,j,0}(n)\epsilon_{1,j,0}(n)$.

The equalization weight with imperfect knowledge of CSI is given by

$$\begin{aligned} w_{j,m}(n) &= Y^*_{j,m} = \bar{H}^*_{0,\bar{j},m}(n)\bar{H}^*_{1,j,m}(n) \\ &= H^*_{0,\bar{j},0}(n)H^*_{1,j,0}(n) + \epsilon^*_y(n), \end{aligned} \quad (29)$$

where $\epsilon_y(n) = H_{0,\bar{j},0}(n)\epsilon_{1,j,0}(n) + H_{1,j,0}(n)\epsilon_{0,\bar{j},0}(n) + \epsilon_{0,\bar{j},0}(n)\epsilon_{1,j,0}(n)$.

B. Derivation of Second Moments

1) Impact of CE Error with Fading Tracking Errors: Using (28) and (29) the second moments can be represented by

$$\begin{cases} g_{xx} = E[|X_{j,m}|^2] = 3\frac{P^2}{\beta^2} + \frac{P^2}{\beta^2}E[|\epsilon_x|^2] - 2\frac{P^2}{\beta^2}J_0^2(2\pi f_d T_s m) \\ +2\left(\frac{P^2}{\beta^2}+1\right)\sigma_n^2, \\ g_{yy} = E[|Y_{j,m}|^2] = E[|H_{sd,m}(n)|^2] + E[|\epsilon_y(n)|^2], \\ g_{xy} = E[X_{j,m}Y^*_{j,m}] = E\left[\frac{P}{\beta} d_{\bar{j},m}(n)H_{sd,m}(n)H^*_{sd,0}(n)\right], \end{cases} \quad (30)$$

while the estimation error variances $E[|\epsilon_x|^2]$ and $E[|\epsilon_y|^2]$ are derived based on the channel estimation error model defined in Sect. III as

$$\begin{aligned} E[|\epsilon_x|^2] &= E[|H_{0,j,0}(n)\epsilon_{1,j,0}(n)|^2] \\ &+ E[H_{0,j,0}(n)\epsilon_{1,j,0}(n)H^*_{1,j,0}(n)\epsilon^*_{0,j,0}(n)] \\ &+ E[H_{0,j,0}(n)\epsilon_{1,j,0}(n)\epsilon^*_{0,j,0}(n)\epsilon^*_{1,j,0}(n)] \\ &+ E[|H_{1,j,0}(n)\epsilon_{0,j,0}(n)|^2] \\ &+ E[H_{1,j,0}(n)\epsilon_{0,j,0}(n)H^*_{0,j,0}(n)\epsilon^*_{1,j,0}(n)] \\ &+ E[H_{1,j,0}(n)\epsilon_{0,j,0}(n)\epsilon^*_{0,j,0}(n)\epsilon^*_{1,j,0}(n)] \\ &+ E[|\epsilon_{0,j,0}(n)\epsilon_{1,j,0}(n)|^2] \\ &+ E[\epsilon_{0,j,0}(n)\epsilon_{1,j,0}(n)H^*_{0,j,0}(n)\epsilon^*_{1,j,0}(n)] \\ &+ E[\epsilon_{0,j,0}(n)\epsilon_{1,j,0}(n)H^*_{1,j,0}(n)\epsilon^*_{0,j,0}(n)] \\ &= 4\sigma_e^2 + 4\sigma_e^4 \end{aligned} \quad (31)$$

and

$$\begin{aligned} E[|\epsilon_y|^2] &= E[|H_{0,\bar{j},0}(n)\epsilon_{1,j,0}(n)|^2] \\ &+ E[H_{0,\bar{j},0}(n)\epsilon_{1,j,0}(n)H^*_{1,j,0}(n)\epsilon^*_{0,\bar{j},0}(n)] \\ &+ E[H_{0,\bar{j},0}(n)\epsilon_{1,j,0}(n)\epsilon^*_{0,\bar{j},0}(n)\epsilon^*_{1,j,0}(n)] \\ &+ E[|H_{1,j,0}(n)\epsilon_{0,\bar{j},0}(n)|^2] \\ &+ E[H_{1,j,0}(n)\epsilon_{0,\bar{j},0}(n)H^*_{0,\bar{j},0}(n)\epsilon^*_{1,j,0}(n)] \\ &+ E[H_{1,j,0}(n)\epsilon_{0,\bar{j},0}(n)\epsilon^*_{0,\bar{j},0}(n)\epsilon^*_{1,j,0}(n)] \\ &+ E[|\epsilon_{0,\bar{j},0}(n)\epsilon_{1,j,0}(n)|^2] \\ &+ E[\epsilon_{0,\bar{j},0}(n)\epsilon_{1,j,0}(n)H^*_{0,\bar{j},0}(n)\epsilon^*_{1,j,0}(n)] \\ &+ E[\epsilon_{0,\bar{j},0}(n)\epsilon_{1,j,0}(n)H^*_{1,j,0}(n)\epsilon^*_{0,\bar{j},0}(n)] \\ &= 4\sigma_e^2 + 4\sigma_e^4. \end{aligned} \quad (32)$$

After substituting (31) and (32) into (30) based on the fading channel modeling [10] in Sect. II-A we obtain the second moments given by (14).

2) 1^{st} Order Interpolation: Factors A_1 and A_2 in (19) are given by

$$\begin{cases} A_1 = -2\left[\left(\frac{M-m}{m}\right)J_0(2\pi f_D T_s m) \right. \\ \left. +\left(\frac{M}{m}\right)J_0(2\pi f_D T_s (M-m))\right]^2 \\ A_2 = \left[\left(\frac{M-m}{m}\right)J_0(2\pi f_D T_s m) \right. \\ \left. +\left(\frac{M}{m}\right)J_0(2\pi f_D T_s (M-m))\right]^2. \end{cases} \quad (33)$$

3) 2^{st} Order Interpolation: Factors A_1 and A_2 in (21) are given by

$$\begin{cases} A_1 = 2\frac{m(m-M)(2M-m)^2}{M^4}J_0(2\pi f_D T_s m)J_0(2\pi f_D T_s (M-m)) \\ +\frac{m(m-M)^2(2M-m)}{M^4}J_0(2\pi f_D T_s m)J_0(2\pi f_D T_s (2M-m)) \\ -2\frac{m^2(m-M)(2M-m)}{M^4}J_0(2\pi f_D T_s (M-m)) \\ \times J_0(2\pi f_D T_s (2M-m)) \\ -\frac{(m-M)^2(2M-m)^2}{2M^4}J_0^2(2\pi f_D T_s m) \\ -2\frac{m^2(2M-m)^2}{M^4}J_0^2(2\pi f_D T_s (M-m)) \\ -\frac{m^2(m-M)^2}{2M^4}J_0^2(2\pi f_D T_s (2M-m)) \\ A_2 = \frac{(m-M)^2(2M-m)^2}{4M^4}J_0^2(2\pi f_D T_s m) \\ +\frac{m^2(2M-m)^2}{M^4}J_0^2(2\pi f_D T_s (M-m)) \\ +\frac{m^2(m-M)^2}{4M^4}J_0^2(2\pi f_D T_s (2M-m)) \\ -\frac{m(m-M)(2M-m)^2}{M^4}J_0(2\pi f_D T_s m)J_0(2\pi f_D T_s (M-m)) \\ -\frac{m(m-M)^2(2M-m)}{2M^4}J_0(2\pi f_D T_s m)J_0(2\pi f_D T_s (2M-m)) \\ +\frac{m^2(m-M)(2M-m)}{M^4}J_0(2\pi f_D T_s (M-m)) \\ \times J_0(2\pi f_D T_s (2M-m)) \\ B_1 = \left[\frac{m^2(m-M)^2(2M-m)^4}{M^8} + \frac{m^4(m-M)^2(2M-m)^2}{M^8} \right. \\ \left. -2\frac{m^3(m-M)^2(2M-m)^3}{M^8}\right]J_0(2\pi f_D T_s M) \\ +\left[2\frac{m^4(m-M)(2M-m)^3}{M^8} \right. \\ \left. -\frac{m(m-M)^3(2M-m)^4}{2M^8} - 2\frac{m^3(m-M)(2M-m)^4}{M^8} \right. \\ \left. +\frac{m^4(m-M)^3(2M-m)}{2M^8} \right. \\ \left. +\frac{m^2(m-M)^3(2M-m)^3}{2M^8} - \frac{m^3(m-M)^3(2M-m)^2}{2M^8}\right](1+2\sigma_e^2) \\ B_2 = \frac{m^2(m-M)^4(2M-m)^2}{4M^8}J_0(2\pi f_D T_s 2M) \\ +\left[\frac{m^2(m-M)^3(2M-m)^3}{M^8} \right. \\ \left. -\frac{m^3(m-M)^3(2M-m)^2}{M^8}\right]J_0^2(2\pi f_D T_s M)J_0(2\pi f_D T_s 2M) \\ -\left[\frac{m(m-M)^4(2M-m)^3}{4M^8} + \frac{m^3(m-M)^2(2M-m)^3}{M^8} \right. \\ \left. +\frac{m^3(m-M)^4(2M-m)}{4M^8}\right](1+2\sigma_e^2). \end{cases} \quad (34)$$

$$\mu = \frac{\frac{P}{\beta} J_0^2(2\pi f_d T_s m)}{\sqrt{\left[3\frac{P^2}{\beta^2} + \frac{P^2}{\beta^2}E[|\epsilon_x|^2] - 2\frac{P^2}{\beta^2}J_0^2(2\pi f_d T_s m) + 2\left(\frac{P^2}{\beta^2}+1\right)\sigma_n^2\right]\left[E[|H_{sd,m}(n)|^2] + E[|\epsilon_y(n)|^2]\right]}}. \quad (35)$$

C. Normalized Covariance

1) Impact of CE Error with Fading Tracking Errors: The normalized covariance is derived by substituting (14) into (11) and it is given by (35) at the top of the page.

Then, by substituting (31) and (32) into (30) and after some manipulation we obtain the normalized covariance given by (11). Finally, using (11) the BER given by (10) and average BER are calculated.

2) Polynomial Interpolation: The same procedure is done for derivation of the normalized covariance and BER expression for polynomial interpolation by substituting (19) and (21) into (11) we obtain the normalized covariance given by (22). Finally, using (22) the BER given by (23) is derived.

REFERENCES

[1] R. W. Yeung, "Multilevel diversity coding with distortion," *IEEE Trans. Inf. Theory*, vol. IT-41, pp. 412–422, 1995.

[2] R. Ahlswede, N. Cai, S.-Y. R. Li, and R. W. Yeung, "Network information flow," *IEEE Trans. Inf. Theory*, vol. 46, pp. 1204–1216, 2000.

[3] S.-Y. R. Li, R. W. Yeung, and N. Cai, "Linear network coding," *IEEE Trans. Inf. Theory*, vol. 49, pp. 371–381, 2003.

[4] P. Popovski and H. Yomo, "Bi-directional amplification of throughput in a wireless multi-hop network," *2006 IEEE Veh. Technol. Conf.*.

[5] S. Zhang, S.-C. Liew, and P. Lam, "Hot topic: physical layer network coding," in *Proc. 2006 ACM MobiCom*, pp. 358–365.

[6] S. Katti, S. S. Gollakota, and D. Katabi, "Embracing wireless interference: analog network coding," *ACM SIGCOM 2007*.

[7] H. Gacanin and F. Adachi, "Broadband analog network coding," *IEEE Trans. Wireless Commun.*, vol. 9, no. 5, pp. 1577–1583, May 2010.

[8] F. Gao, R. Zhang, and Y.-C. Liang, "On channel estimation for amplify-and-forward two-way relay networks," *2008 IEEE Global Commun. Conf.*

[9] T. Sjodin, H. Gacanin, and F. Adachi, "Two-slot channel estimation for analog network coding based on OFDM in a frequency-selective fading channel," *2010 IEEE Veh. Technol. Conf. – Spring*,.

[10] W. C. Jakes, *Microwave Mobile Communications*, 2nd edition. IEEE Press, 1993.

[11] J. G. Proakis, *Digital Communications*, 3rd edition. McGraw-Hill, 1995.

[12] H. Gacanin, M. Salmela, and F. Adachi, "Bit error rate analysis for wireless network coding with imperfect channel state information," *2010 IEEE International Conf. Commun. Syst.*

Haris Gacanin was born in Sarajevo, Bosnia and Herzegovina, where he received his Dipl.-Ing. degree in Electrical engineering from the Faculty of Electrical Engineering, University of Sarajevo in 2000. He received his M.E.E. and Ph.D.E.E. from Graduate School of Electrical Engineering, Tohoku University, Japan, in 2005 and 2008, respectively. Since April 2008 until May 2010 he has been working first as Japan Society for Promotion of Science (JSPS) postdoctoral research fellow and then as an Assistant Professor at Graduate School of Engineering, Tohoku University. Currently, he is with Alcatel-Lucent Bell N.V. in Antwerp, Belgium. His research interest is in the fields of wireline and wireless communications with focus on: home networking technology and architectures, management and diagnostics of home and access networks, xDSL transmission technology, wireless network coding, channel estimation and equalization, cognitive radio, MIMO, wireless sensor networks, dynamic resource allocation, iterative receivers, channel coding and hybrid ARQ, PAPR reduction, cooperative relaying, communication theory and gigabit PON identification. He is member of IEEE and IEICE and Chair of the IEICE Europe Section. He was acting as a chair, review and technical program committee member of various technical journals and conferences. He is a recipient of the 2010 KDDI Foundation Research Grant Award, the 2008 Japan Society for Promotion of Science (JSPS) Postdoctoral Fellowships for Foreign Researchers, the 2005 Active Research Award in Radio Communications, 2005 Vehicular Technology Conference (VTC 2005-Fall) Student Paper Award from IEEE VTS Japan Chapter and the 2004 Institute of IEICE Society Young Researcher Award. He was awarded by Japanese Government (MEXT) Research Scholarship in 2002.

Mika Salmela received his M.S. degree in electrical engineering from Aalto University School of Science and Technology, Espoo, Finland, in 2010. During Apr. 2009-Mar. 2010 he studied in Adachi Lab, Tohoku University, Japan and was a research student of the DEEP program. His research interests include channel estimation and equalization techniques with particular application to mobile communication systems.

Fumiyuki Adachi received the B.S. and Dr. Eng. degrees in electrical engineering from Tohoku University, Sendai, Japan, in 1973 and 1984, respectively. In April 1973, he joined NTT Laboratories and conducted various types of research related to digital cellular mobile communications. From July 1992 to December 1999, he was with NTT DoCoMo, Inc., where he led a research group on W-CDMA for 3G systems. Since January 2000, he has been with Tohoku University, Sendai, Japan, where he is a Professor of Electrical and Communication Engineering at the Graduate School of Engineering. His research interests are in gigabit wireless signal processing and networking including wireless access, equalization, transmit/receive antenna diversity, equalization, channel coding, and distributed MIMO signal processing. He has published over 500 papers in journals and conference proceedings. He is an IEEE Fellow and an IEICE Fellow. He was a recipient of the IEEE Vehicular Technology Society Avant Garde Award 2000, IEICE Achievement Award 2002, Thomson Scientific Research Front Award 2004, Ericsson Telecommunications Award 2008, Telecom System Technology Award 2010, and Prime Minister Invention Prize 2010.